Strong correlation effects in the electronic structure of Sr$_2$FeMoO$_6$

Sugata Ray,[1] Priya Mahadevan,[1,2] Ashwani Kumar,[1] D. D. Sarma,[1,*] R. Cimino,[3] M. Pedio,[4] L. Ferrari,[4] and A. Pesci[5]

[1]*Solid State and Structural Chemistry Unit, Indian Institute of Science, Bangalore 560 012, India*
[2]*National Renewable Energy Laboratory, Golden, Colorado 80401*
[3]*LNF-INFN V. E. Fermi 40 I-00044 Frascati (Roma), Italy*
[4]*ISM-CNR sede distaccata Trieste S.S. 14, Km. 163.5 I-34012 Basovizza (TS), Italy*
[5]*University of Trieste, Trieste, Italy*

We investigate the electronic structure of Sr$_2$FeMoO$_6$ combining photoemission spectroscopy with a wide range of photon energies and electronic structure calculations based on first-principle as well as model Hamiltonian approaches to reveal several interesting aspects. We find evidence for unusually strong Coulomb correlation effects both in the Fe $3d$ *and* O $2p$ states, with an enhanced manifestation in the majority spin channel. Additionally, O $2p$ states exhibit a spin splitting of nonmagnetic origin, which nevertheless is likely to have a subtle influence on the stability of the ferromagnetism of this compound.

INTRODUCTION

Sr$_2$FeMoO$_6$ was recently shown to exhibit a pronounced negative magnetoresistance at higher temperatures and lower magnetic fields[1] compared to the manganites, making it intrinsically more suitable for technological applications. An essential aspect of understanding the properties of this material is to understand the underlying electronic structure. The basic ingredient for crystal structure of this material is the cubic perovskite structure, with Fe and Mo alternating in the (100), (010), and (001) directions. As in the case of the other ABO$_3$ perovskites, where A is an alkali-metal atom and B is a transition metal atom, the valence and conduction bands of Sr$_2$FeMoO$_6$ involve the d states of the two transition metal atoms Fe and Mo, besides the oxygen p states. It was recently shown[2−4] that the Mo $4d$–O $2p$ hybridized states play a crucial role in establishing the unusually high magnetic ordering temperature in Sr$_2$FeMoO$_6$ via a mechanism that relies on the location of these Mo $4d$–O $2p$ hybridized states energetically between the exchange-split Fe states. There has been only one direct investigation[5] of the electronic structure of this compound so far, with another investigation[6] reporting on a related compound, Ba$_2$FeMoO$_6$. These experimental results suggest a substantial disagreement with *ab initio* band structure results and are interpreted in terms of local density approximation (LDA)+U calculations by incorporating Coulomb interactions within the Fe $3d$ manifold. We have performed photoemission experiments on Sr$_2$FeMoO$_6$ and Sr$_2$FeMo$_x$W$_{1−x}$O$_6$ with a photon energy range that encompasses the combined range of the previous two experiments, farther extended by including photoemission results with x-rays. These detailed experimental results are analyzed in conjunction with calculations based on multiband Hubbard model within a mean-field decoupling of the interaction terms as well as *ab initio* approaches.

We identify the origin of various features in the experimental valence band spectrum with the help of the dependence of the matrix elements on the photon energy. Thus we find that while the specific ordering of energy levels near the Fermi energy, crucial for the magnetism, is in agreement with the *ab initio* results, there are some significant differences between the experimental and the *ab initio* results in agreement with previous reports, indicating the presence of strong correlation effects. Moreover, we show that the conventional LDA+U and parametrized model Hamiltonian approaches are also in disagreement with the experimental results in certain details, particularly in the spectral range dominated by oxygen p states, though the inclusion of U_{dd} improves the description of Fe d related spectral features, as also observed previously. It turns out that the inclusion of the interaction terms within the oxygen p states improves the agreement between the calculated results and the experiment. We further establish a few unusual aspects of the electronic structure in this compound specifically related to the O p band, such as a spin splitting of nonmagnetic origin. These findings are possibly of importance in understanding the stability of the ferromagnetic state and provide a clue why the magnetic structure in this compound was recently found to depend critically on factors that influence the O p states.[7,8]

EXPERIMENT

Polycrystalline Sr$_2$FeMoO$_6$ was prepared by standard solid state route as described in Ref. 1. Stoichiometric amounts of SrCO$_3$, MoO$_3$, and Fe$_2$O$_3$ were mixed thoroughly and heated at 900 °C in air for 3 h. The fully oxidized black powder is then grounded and pelletized into 10-mm-diameter pellets of 2-mm thickness. These pellets were then annealed at 1200 °C in a flowing gas mixture of ∼10% H$_2$/Ar for 5 h. X-ray diffraction (XRD) experiments on this powder confirmed the presence of highly ordered (i.e., near perfect alternate occupancy of Fe and Mo ions along the three cubic axes) and pure double perovskite Sr$_2$FeMoO$_6$ phase. It has a tetragonal I4/*mmm* space group with $a=b$ = 10.5229 a.u. and $c=$14.9236 a.u.; Sr, Fe, Mo, O1, and O2 sites occupy 8g, 4e, 4e, 4e, and 8h positions, respectively.

A different method was used for synthesizing W-doped Sr$_2$FeMoO$_6$ samples, because it was otherwise not possible to entirely get rid of SrMoO$_4$/SrWO$_4$-type oxidized impurities, whenever the W-doped samples were synthesized by the above mentioned procedure. Therefore, all the W-doped samples were first prepared by melt-quenching method;[9] the

technique which always produced slightly less ordered but highly pure samples. These pellets were crushed, ground, thoroughly and finally annealed at the same condition in the form of pellets in order to achieve maximum ordering.[10] The purity and chemical homogeneity of the final products were checked by XRD and energy dispersive analysis of x ray (EDAX) techniques.

Majority of the photoemission experiments were carried out at the vacuum ultraviolet photoemission beamline, 3.2R at Synchrotron Radiation Center, Elettra, Trieste, with a sample temperature of 77 K. The sample surface was cleaned by *in situ* scraping with a diamond file. Valence band spectrum using x-ray photoemission spectroscopy (XPS) was recorded in a standard VSW electron spectrometer[11] at $\sim$120 K with monochromatized Al$K\alpha$ radiation.

CALCULATIONAL METHODS

The *ab-initio* band structure of Sr_2FeMoO_6 was computed using both the LMTO-ASA method using the Perdew Wang generalized gradient approximation (GGA) exchange functional[12] and the plane wave pseudopotential method. No empty spheres were introduced, and the volume filling criterion was satisfied with less than 16% overlap between the spheres in the linearized muffin-tin orbital (LMTO) method with the atomic sphere approximation (ASA) calculations. Ultrasoft pseudopotentials[13] as implemented in VASP,[14] were used for the calculations performed with a plane wave cutoff of 20 Ry and the accuracy of our conclusions was checked by increasing the plane wave cutoff to 25 Ry. Both the internal as well as the external cell parameters were optimized. The GGA (Ref. 12) optimized lattice constants were 10.59 and 14.997 a.u. and the optimized internal coordinates were Sr $(8g)$ $z=0.25$, Fe $(4e)$ $z=0$, Mo $(4e)$ $z=0.5$, O1 $(4e)$ $z=0.2527$, and O2 $(8h)$ $x=0.2474$, in agreement with the experimental parameters.

The band structure obtained from both *ab initio* methods were found to be in agreement. We fit the magnetic band structure along various symmetry directions with band dispersions within a nearest neighbor tight binding model[15] in order to obtain estimates of the hopping parameters for the use in the multiband Hubbard model. The basis of the tight-binding Hamiltonian includes d orbitals on Fe and Mo atoms as well as p orbitals on oxygen. As the Sr states do not contribute in the energy window that we are interested in, the basis of the tight binding model does not include states on the Sr atoms. The tight binding model considered includes hopping between oxygen atoms, as well as between Fe and oxygen and Mo and oxygen; these interaction strengths[16] are given in terms of the Slater-Koster parametrization. Instead of using different onsite energies (ϵ_i) for up and down spin orbitals to describe the magnetic structure as in the past,[15] we replace the different on-site energies for the up and down spin of Fe by an on-site direct Coulomb (U_{dd}) interaction strength of 3 eV and a Hund's exchange coupling (J) strength of 0.7 eV on the Fe site as appropriate[15] for Fe^{3+} oxide systems; this method allows us to solve for the changes in the energies of the Fe $3d$ level as a result of direct and exchange Coulomb interactions self-consistently. Besides the
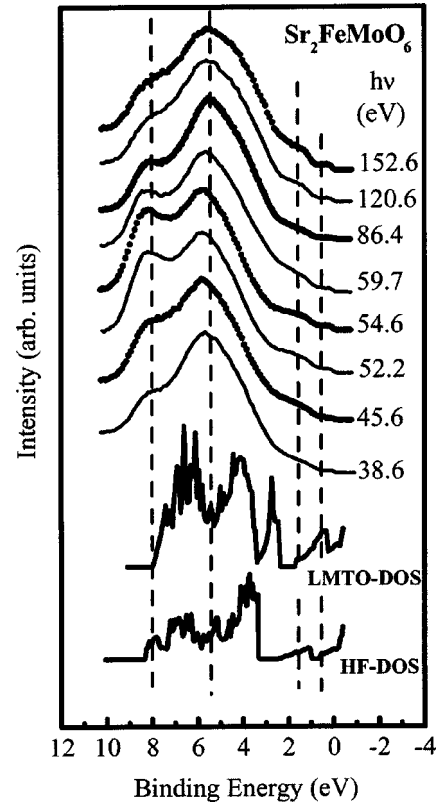

FIG. 1. Valence band spectra of Sr_2FeMoO_6 with different $h\nu$ compared with the calculated DOS using LMTO-ASA and Hartree-Fock approaches with finite U_{dd}.

usual one-body tight binding part, the Hamiltonian includes the intrasite Coulomb interaction term at the Fe site in the form $(U_{dd}-J\delta_{\sigma_1,\sigma_2})n_{\alpha_1,\sigma_1}n_{\alpha_2,\sigma_2}$, where α_i denotes the five $3d$ orbitals on the Fe site and σ_i denotes the spin. As discussed later in the text, certain features in the experimental spectra prompted us to include an additional term representating Coulomb interactions within the oxygen p orbitals in the form $U_{pp} n_{\beta_1,\sigma} n_{\beta_2,\sigma'}$. The effect of such a term involving U_{pp} was studied in the context of the electronic structure of the high temperature superconductors[17] and other oxide systems.[18] The four fermion terms in the Hamiltonian were decoupled by using a mean-field approximation.[19] The decoupled Hamiltonian involved the occupancies of various orbitals, which were then solved selfconsistently over a k mesh of 1000 k points.

RESULTS AND DISCUSSION

In Fig. 1 we show a selection of the valence band photoemission spectra of Sr_2FeMoO_6, obtained using different incident photon energies. All the spectra exhibit a finite intensity at E_F, in agreement with the metallic behavior in this compound. For comparison, we also show the calculated total density of states (DOS) for fully ordered Sr_2FeMoO_6, obtained within spin-polarized LMTO-ASA band structure calculation with the generalized gradient approximation over the relevant energy range just below the experimental spectra. The experimental spectra show four distinct features, appearing at about 0.4, 1.8, 5.6, and 8.3 eV binding energies,

marked by the vertical dotted lines in Fig. 1. The calculated LMTO-DOS clearly does not agree with the measured spectra, with the calculation suggesting regions of low DOS at three of these energies, namely, at 1.8, 5.6, and 8.3 eV. In particular, the remarkably intense feature at 8.3 eV in the experimental spectra lies outside the calculated bandwidth. This is similar to the cases of U intermetallics[20] and transition metal oxides, such as NiO,[21] exhibiting correlation-driven large spectral weights, or even distinct peaks, outside the calculated bandwidth. It is significant to note that this correlation driven satellite in Sr_2FeMoO_6 is very intense and is undoubtedly the highest among all Fe^{3+} oxides studied so far;[22,23] for example, it is known[23] that spectroscopic data on $LaFeO_3$, a closely related perovskite oxide with Fe^{3+}, can be reasonably well described within *ab initio* approaches.

A standard route to take into account the effect of Coulomb interactions on the band structure is to incorporate this interaction within the transition metal $3d$ manifold in a mean-field sense, as in the case of LDA+U approach or the Hartree-Fock (HF) type mean-field approach described for the multiband Hubbard model in the previous section. It is indeed true that such approaches have proved to be very useful for describing transition metal compounds. We show the total density of states obtained within the HF treatment of the multiband Hamiltonian including Coulomb interactions only at the Fe sites at the bottom of Fig. 1; our result is in agreement with LDA+U results.[3,5,6,8] A comparison of the experimental data with the two calculations (LMTO and HF) readily suggests that the HF-type approach with the multiband model provides a better agreement with the experiment in comparison to the LMTO-GGA results. Specifically, the experimentally observed 1.8-eV feature and the satellite structure at about 8 eV, outside the GGA-derived bandwidth, have corresponding features in the model Hamiltonian results. Interestingly, however, the sharp disagreement between the most intense feature in the 5–6-eV range in the experimental spectrum and the deep valley of low calculated DOS in the same energy range continues to exist in the HF-DOS, just as in the LMTO-DOS. The same discrepency can also be observed in the LDA+U results compared with experimental results, reported in Refs. 5, 6 and 8 though this disagreement has not been commented up on so far.

Before attempting to understand the origin of this discrepency, we first establish the origin of various experimental features from the dependencies of the normalized spectral intensities on the photon energies [Figs. 2(a) and 2(b)]. We found that the two features appearing at 1.8 and 8.3 eV exhibit a significant nonmonotonic $h\nu$ dependence in the range of 42–65 eV [Fig. 2(a)], spanning the Fe $3p$ absorption threshold near 55 eV. Such a resonance phenomenon clearly establishes substantial Fe $3d$ contributions in these states. More interestingly, the nature of the dependencies is different for the two features. The 8.3-eV feature exhibits a clear maximum, indicating about a 30% resonant enhancement, characteristic of such correlation driven satellite or incoherent features. We have found almost identical variations in the satellite features in closely related W-substituted compounds also, as shown in the figure. In contrast, the 1.8-eV feature shows approximately a 20% dip in the intensity near the on-resonant condition, as is characteristic of more bandlike or coherent features.[24]
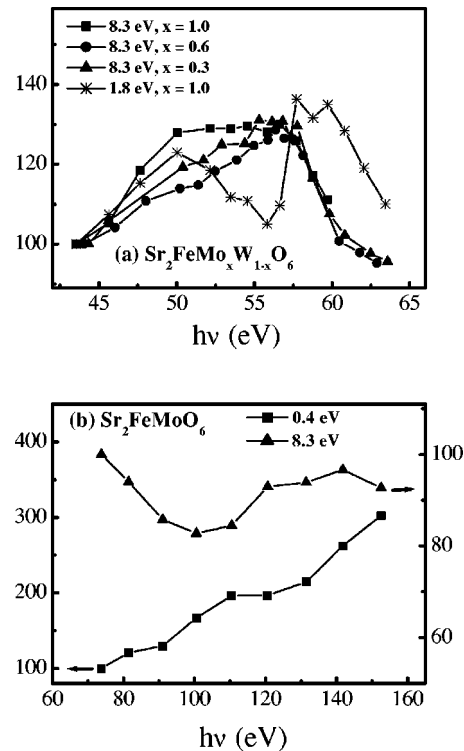

FIG. 2. Percentage variation in the relative intensities of various spectral features in the valence band spectra as a function of photon energy (a) between 45 and 65 eV for $Sr_2FeMo_xW_{1-x}O_6$; and parent Sr_2FeMoO_6 and (b) between 70 and 152 eV for Sr_2FeMoO_6. All intensities are normalized with the intensity of the most intense peak at 5.6 eV, almost fully contributed by O p states. The normalized intensity of each feature recorded with the lowest $h\nu$ is always scaled to 100% in order to emphasize the variation in the relative intensity of various features with $h\nu$.

In order to identify the states with dominant Mo contributions, we plot the normalized intensities of the features at the E_F and 8.3 eV for $h\nu$ between 75 and 152 eV in Fig. 2(b). This photon energy range is most suitable for the purpose, since there is a minimum (called the Cooper minimum) in the cross-section of localized Mo $4d$ related intensities in solids at about $h\nu \sim 100-110$ eV.[25] Fig. 2(b) clearly shows a significant minimum in the relative intensity of the 8.3-eV feature (triangles) at about $h\nu \sim 100$ eV, exactly where the Cooper minimum for the localized Mo $4d$ states are expected. This establishes that the Mo $4d$ states also contribute significantly to the 8-eV spectral region. In contrast to the behavior of the localized states, delocalized bandlike Mo d states, however, do not exhibit any Cooper minimum.[25] Therefore, the relative intensity of Mo $4d$ delocalized states compared to the O $2p$ states is expected to show a rapid, monotonic increase with increasing photon energy $h\nu$, due to the changes in the relative Mo $4d$–O $2p$ cross sections.[26] Such an increasing trend is indeed exhibited by the relative intensity of the feature at E_F [see the square data in Fig. 2(b)], establishing a dominant contribution from *delocalized* Mo $4d$ states in this energy region.

The assignment of various spectral features is further confirmed by a comparison of the intensity variations when the photon energy is changed from $h\nu < 100$ eV to 1486.6 eV
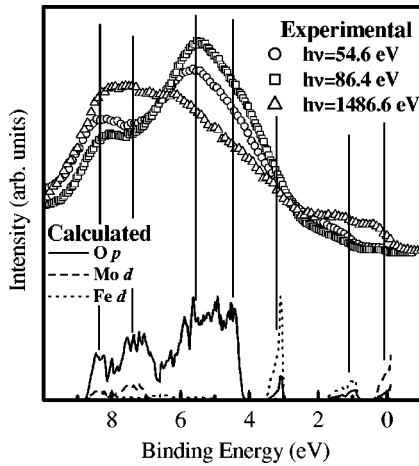
FIG. 3. Normalized valence band spectra of Sr_2FeMoO_6 with $h\nu = 54.6$, 86.4, and 1486.6 eV; spin integrated partial O $2p$ (solid line), Mo $4d$ (dashed line), and Fe $3d$ (short dashed line) DOSs obtained by Hartree-Fock calculations including U_{pp} in addition to U_{dd} are shown at the bottom. Different spectral features are marked by vertical thin lines.

using AlKα radiation. In Fig. 3 we show these spectra with the integrated area being normalized for each spectrum, with two representative low photon energy spectra with $h\nu = 54.6$ eV (open circles) and $h\nu = 86.4$ eV (open squares), while the x-ray photoelectron spectrum (shown with open triangles in Fig. 3) with $h\nu = 1486.6$ eV. It is evident from this comparison that there are substantial changes in the spectral intensities of various features, as the photon energy is changed by ~ 1400 eV, thereby changing the relative cross sections of various states drastically. The most obvious spectral changes are the very strong increases in the intensities of features near E_F and in the 7–9-eV range, substantial increase in the intensity of the feature at 1.8 eV and a decrease in the energy region 4–6-eV binding energy in the high photon energy XP spectrum. Noting that the Mo $4d$ cross-section increases strongly and that of Fe $3d$ moderately relative to the oxygen $2p$ states, we may attribute substantial Mo $4d$ contributions in the near E_F and 7–9-eV binding energy region, primary Fe $3d$ contribution in the 1.8 eV region and a dominance of O $2p$ derived states in the 4–6-eV binding energy. These conclusions are in agreement with the interpretation based on the spectral changes within the low photon energy ($h\nu < 200$ eV) range [see Figs. 2(a) and 2(b)]. Figure 2 also establishes substantial localized Fe $3d$ contributions in the neighborhood of the 8.3-eV feature, in addition to the Mo $4d$ contribution. These assignments of the spectral features at once provide us with an understanding of both the partial success and the specific failure of the mean-field calculated results (HF-DOS) as well as LDA+U results reported earlier,[3,5,6,8] to explain the experimental spectral features. Compared to the GGA, the incorporation of Coulomb interaction within the Fe $3d$ manifold in terms of these mean-field approaches improves the agreement between the experiment and the calculation for the 1.8- and 8.3-eV features that have significant Fe $3d$ character (see Fig. 1); the 8.3 eV feature also attains substantial Mo $4d$

character due to large hopping interactions present in the system. However, at this level of mean-field approximation, there is still a rather pronounced disagreement between the experiment and calculation in the 4–6-eV energy range;[27] our experimental results have already established that this energy region is dominated by O p states. Thus a single-particle approach for the O p states fails to describe the experiment, while the average effect of Coulomb interactions within Fe $3d$ states improve the description of the Fe $3d$ related features; this suggests a possible role of Coulomb interactions also within the O p states. This is not altogether surprising, since it is known from analysis of the *KLL* Auger spectra for O in transition metal oxides[28,29] that the Coulomb interaction strength U_{pp} in the O p states is comparable to the Coulomb interaction strength in the transition metal $3d$ states. While U_{pp} is not often explicitly used in various approaches to describe the electronic structure of transition metal oxides, as in the LDA+U method applied so far to Sr_2FeMoO_6 or the preceeding mean-field results presented in this paper, there are some applications of models including the U_{pp} term,[17,18] most notably in the case of copper compounds with a substantial p admixed character of the charge carriers. Since the charge carriers in Sr_2FeMoO_6 have a significantly admixed Mo $4d$–O $2p$ character,[4] it is reasonable to anticipate a possible role of U_{pp} in the present system also, thus suggesting an explanation for the disagreement between the experimental spectra and the calculated results with U_{dd} alone. Therefore, we included the U_{pp} term in the multiband Hubbard model and calculated the total and partial densities of states within the mean-field approximation; we found that the inclusion of $U_{pp} = 3.8$ eV improves the agreement between the experiment and the calculation substantially, primarily via a renormalization of oxygen related site energies. The agreement improves further with an enhancement of the splitting of O p up- and down-spin bare energies, from the value (0.4 eV) estimated from *ab initio* band structure results, to 0.7 eV; the resulting Fe d, Mo d, and O p
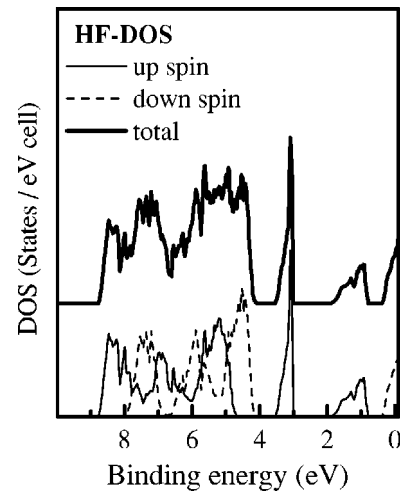

FIG. 4. Total DOS obtained by Hatree-Fock calculations including U_{pp} in addition to U_{dd} (thick solid line). The up (thin solid line) and down (dashed line) spin DOSs are also shown at the bottom of the panel.
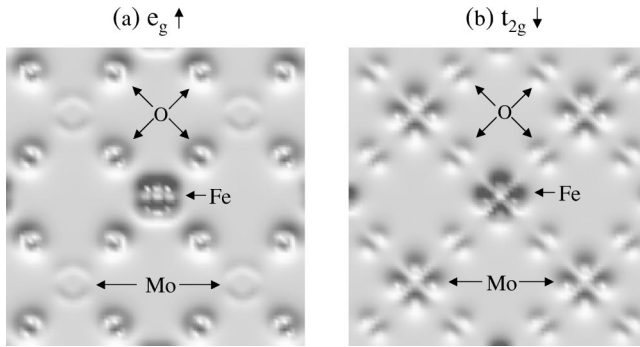
FIG. 5. Charge density plots in the basal plane for (a) $e_{g\uparrow}$ states in the energy window E_F-2 eV to E_F and (b) $t_{2g\downarrow}$ states in the energy window E_F-1 to E_F+0.5 eV.

partial DOSs are compared with experimental spectra in Fig. 3. Specifically, the dip in the HF-DOS with $U_{pp}=0$ as well as in GGA results (Fig. 1) in the energy range of 4–6 eV is replaced with a large intensity feature in the presence of U_{pp}, in agreement with the experimentally observed broad maximum. We also find that the partial contributions from Mo $4d$, Fe $3d$, and O $2p$ states in different energy regions are in good agreement with experimental results. Thus the calculation shows a dominant Mo $4d$ contribution due to t_{2g} states at E_F, with significant contributions of t_{2g} and e_g symmetries in the energy range of 7–9 eV; dominant Fe $3d$ contributions at 1.5- and 3-eV binding energy regions, arising from e_g and t_{2g} states respectively, with a significant intensity contribution in the satellite region of 8–9 eV; and a dominant O $2p$ nonbonding contribution in the 4–6-eV binding energy.

Spin-polarized DOSs along with the total DOS, shown in Fig. 4, establish some interesting features in the electronic structure of this compound. First, the spectral feature appearing near 8.3 eV, outside the GGA calculated bandwidth and associated with a correlation-driven satellite, is entirely contributed by the up-spin channel, suggesting a more pronounced localized nature of electron states in this spin channel compared to the down-spin channel. This result can be understood in terms of the half-metallic nature of the ground state with the up-spin channel indeed localized with a gap at E_F, while the down-spin channel is delocalized with a finite DOS at E_F. However, a gap at the E_F does not necessarily imply a localization of the wave function in space; we confirm the localized-in-space nature of the up-spin channel in contrast to the down-spin channel by plotting the charge densities of the $e_{g\uparrow}$ and $t_{2g\downarrow}$ spin states close to E_F in the basal

plane of the unit cell in Fig. 5. This figure [Fig. 5(b)] shows the extended nature of the down-spin charge density with substantial weights on all atomic sites, namely, Fe, O and Mo. In clear contrast, the up-spin charge density [Fig. 5(a)] has virtually no contribution on Mo; consequently, the charge density plot suggests almost completely localized charge densities decoupled and isolated on individual FeO$_6$ octahedra.

We have already pointed out that an analysis of the *ab initio* band structure results suggests a splitting of about 0.4 eV between the oxen up- and down-spin p states, and that a proper simulation of the experimental spectra required a further enhancement of this splitting to 0.7 eV within the HF approach. This is an unusually large spin-splitting compared to oxygen p states in other ferromagnetic oxide systems. One explanation for the spin splitting could be based on the atomic exchange strength. However, since the exchange splitting is given by the product of the moment and the exchange strength and the typical oxygen moment in this compound is less than $0.1\mu_B$,[30] this explanation would require an unphysically large exchange strength at the oxygen sites. We have traced back the nonmagnetic origin of this spin splitting to the differing spatial extents of the corresponding oxygen charge densities in up- and down-spin channels. The overall behavior of the charge densities in the two spin channels are grossly similar and a direct comparison of the two will not show any remarkable difference. In order to enhance the contrasting behaviors between the two spin channels, we construct the charge density difference between the two spin channels. In Fig. 6 we plot this difference in up- and down-spin charge densities in the basal plane. We show the positive part of the (up-$down$) charge density in the left panel and the complementary ($down$-up) one in the right panel. Thus the left panel shows the space region with a higher charge density in the up-spin channel compared to the down-spin channel, and the right one shows the excess charge density in the down-spin channel compared to the up-spin channel. It is clear from the figure that the down-spin channel of oxygen p states are spatially more extended than the up-spin states, with the spatial extension more dominantly in the direction of perpendicular bisector of the Fe-O-Mo bond through the O site. We have analyzed several states within the oxygen nonbonding region; all of them show the common features of a more extended down-spin channel with relatively more charge density away from the nearby positively charged metal centers compared to the up-spin channel. This shows that the crystal-field stabilization of the electron states due to the positively charged neighboring sites will be relatively
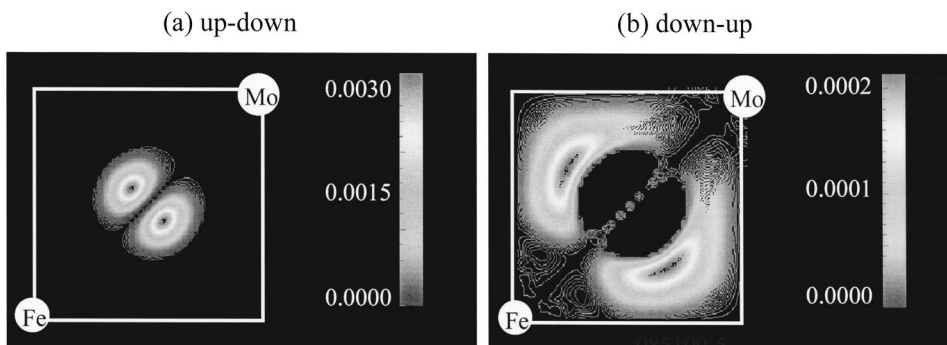

FIG. 6. Plots of differences in charge densities [(a) up-down and (b) down-up)] of the oxygen nonbonding states at the Γ point in the basal plane. The oxygen site (not marked) is situated approximately halfway between Mo and Fe.

greater for the up-spin oxygen states compared to the down-spin ones, as indeed found here, giving rise to the apparent exchange splitting of the oxygen p states.

In conclusion, we have found that the electronic structure of Sr_2FeMoO_6 is dominated by strong electron correlation effects, manifesting more prominently within the Fe $3d$ up-spin states, as a consequence of its half-metallic ground state. A detailed analysis of the spectral features using photon energy variation allows us to establish two interesting effects related to the oxygen p states. First, it appears necessary to explicitly account for the Coulomb interactions within the oxygen p states, and, second, there is a splitting between the oxygen p up- and down-spin channels arising from different spatial extensions of the corresponding wave functions. In this context, we note that the ferromagnetic stability in Sr_2FeMoO_6 is sensitively dependent on the properties of oxygen states and the first principle band structure calculations tend to underestimate the ferromagnetic stability.[7,8] Our findings here are likely to provide an understanding of the stability of ferromagnetism in this system, as our preliminary calculation of the spin wave dispersions indicates that the ferromagnetism is indeed favored by both finite U_{pp} and the "spin" splitting of the oxygen p states.

*Also at Jawaharlal Nehru Center for Advanced Scientific Research, Bangalore, India. Email address: sarma@sscu.iisc.ernet.in

[1] K.-I. Kobayashi, T. Kimura, H. Sawada, K. Terakura, and Y. Tokura, Nature (London) **395**, 677 (1998).

[2] D. D. Sarma, Priya Mahadevan, T. Saha-Dasgupta, Sugata Ray, and Ashwani Kumar, Phys. Rev. Lett. **85**, 2549 (2000); Sugata Ray, Ashwani Kumar, D. D. Sarma, R. Cimino, S. Turchini, S. Zennaro, and N. Zema, *ibid.* **87**, 097204 (2001).

[3] J. Kanamori and K. Terakura, J. Phys. Soc. Jpn. **70**, 1433 (2001); Z. Fang, K. Terakura, and J. Kanamori, Phys. Rev. B **63**, 180407(R) (2001).

[4] D. D. Sarma, Curr. Opin. Solid State Mater. Sci. **5**, 261 (2001).

[5] T. Saitoh, M. Nakatake, A. Kakizaki, H. Nakajima, O. Morimoto, Sh. Xu, Y. Moritomo, N. Hamada, and Y. Aiura, Phys. Rev. B **66**, 035112 (2002).

[6] J.-S. Kang, H. Han, B. W. Lee, C. G. Olson, S. W. Han, K. H. Kim, J. I. Jeong, J. H. Park, and B. I. Min, Phys. Rev. B **64**, 024429 (2001).

[7] K. Terakura (private communication).

[8] N. Hamada (private communication).

[9] D. D. Sarma, E. V. Sampathkumaran, Sugata Ray, R. Nagarajan, Subham Majumdar, Ashwani Kumar, G. Nalini, and T. N. Guru Row, Solid State Commun. **114**, 465 (2000).

[10] Sugata Ray, Ashwani Kumar, Subham Majumdar, E. V. Sampathkumaran, and D. D. Sarma, J. Phys.: Condens. Matter **13**, 607 (2001).

[11] S. R. Krishnakumar, T. Saha-Dasgupta, N. Shanthi, Priya Mahadevan, and D. D. Sarma, Phys. Rev. B **63**, 045111 (2001).

[12] John P. Perdew and Yue Wang, Phys. Rev. B **45**, 13 244 (1992).

[13] D. Vanderbilt, Phys. Rev. B **41**, 7892 (1990).

[14] G. Kresse and J. Furthmüller, Phys. Rev. B **54**, 11 169 (1996); G. Kresse and J. Furthmüller, Comput. Mater. Sci. **6**, 15 (1996).

[15] P. Mahadevan, N. Shanthi, and D. D. Sarma, Phys. Rev. B **54**, 11 199 (1996); Priya Mahadevan, N. Shanthi, and D. D. Sarma, J. Phys.: Condens. Matter **9**, 3129 (1997); Priya Mahadevan and D. D. Sarma, Phys. Rev. B **61**, 7402 (2000).

[16] The electronic parameters obtained from the tight-binding fitting of the *ab initio* band dispersions in eV are $pd\sigma$(Fe-O) = -1.9 (-2.1), $pd\pi$(Fe-O) = 0.72 (1.11), $pd\sigma$(Mo-O) = -2.58 (-2.66), $pd\pi$(Mo-O) = 1.74 (1.62), $pp\sigma$(O-O) = 0.45 (0.35), and $pp\pi$ = 0.02 (-0.02) along with onsite energies of -4.46 (-4.03), -1.39 (-1.68), 2.17 (1.82), -3.46 (-3.03), and -2.96 (-2.12) for up (down) spin orbitals of O p, Mo t_{2g}, Mo e_g, Fe t_{2g}, and Fe e_g orbitals, respectively.

[17] V. I. Belinicher and A. L. Chernyshev, Phys. Rev. B **49**, 9746 (1994).

[18] I. A. Nekrasov, M. A. Korotin, and V. I. Anisimov, cond-mat/0009107 (unpublished).

[19] D. D. Sarma, H. R. Krishnamurthy, Seva Nimkar, S. Ramasesha, P. P. Mitra, and T. V. Ramakrishnan, Pramana, J. Phys. **38**, L531 (1992); Seva Nimkar, D. D. Sarma, H. R. Krishnamurthy, and S. Ramasesha, Phys. Rev. B **48**, 7355 (1993); P. Mahadevan, K. Sheshadri, D. D. Sarma, H. R. Krishnamurthy, and Rahul Pandit, *ibid.* **55**, 9203 (1997).

[20] J. W. Allen, S.-J. Oh, L. E. Cox, W. P. Ellis, M. S. Wire, Z. Fisk, J. L. Smith, B. B. Pate, I. Lindau, and A. J. Arko, Phys. Rev. Lett. **54**, 2635 (1985); D. D. Sarma, F. U. Hillebrecht, W. Speier, N. Mårtensson, and D. D. Koelling, *ibid.* **57**, 2215 (1986).

[21] A. Fujimori, F. Minami, and S. Sugano, Phys. Rev. B **29**, 5225 (1984).

[22] A. Chainani, M. Mathew, and D. D. Sarma, Phys. Rev. B **48**, 14 818 (1993).

[23] D. D. Sarma, N. Shanthi, S. R. Barman, N. Hamada, H. Sawada, and K. Terakura, Phys. Rev. Lett. **75**, 1126 (1995); D. D. Sarma, N. Shanthi, and P. Mahadevan, Phys. Rev. B **54**, 1622 (1996).

[24] A. Fujimori, K. Mamiya, T. Mizokawa, T. Miyadai, T. Sekiguchi, H. Takahashi, N. Môri, and S. Suga, Phys. Rev. B **54**, 16 329 (1996); K.-H. Walker, E. Kisker, C. Carbone, and R. Clauberg, *ibid.* **35**, 1616 (1987).

[25] I. Abbati, L. Braicovich, C. Carbone, J. Nogami, J. J. Yeh, I. Lindau, and U. del Pennino, Phys. Rev. B **32**, 5459 (1985).

[26] J. J. Yeh and I. Lindau, At. Data Nucl. Data Tables **32**, 1 (1985).

[27] This disagreement is less visible in a comparison between XPS spectrum and HF results due to a suppression of photoemission cross-section of O p states at higher photon energies.

[28] J. Ghijsen, L. H. Tjeng, J. van Elp, H. Eskes, J. Westerink, G. A. Sawatzky, and M. T. Czyzyk, Phys. Rev. B **38**, 11 322 (1988).

[29] A. Chainani, M. Mathew, and D. D. Sarma, Phys. Rev. B **46**, 9976 (1992); A. Chainani, M. Mathew, and D. D. Sarma, *ibid.* **47**, 15 397 (1993); A. Chainani, M. Mathew, and D. D. Sarma, *ibid.* **48**, 14 818 (1993).

[30] T. Saha-Dasgupta and D. D. Sarma, Phys. Rev. B **64**, 064408 (2001).